

Studies of the sea surface by short – range radar IKI-2M in distance–time regime

Badania powierzchni morza za pomocą radaru krótkiego zasięgu IKI-2M w reżimie „odległość–czas”

Yu.A. Kravtsov¹, M.D. Raev², E.I. Skvortsov²

¹ Maritime University of Szczecin, Institute of Physics
Akademia Morska w Szczecinie, 70-500 Szczecin, Wały Chrobrego 1–2
e-mail: y.kravtsov@ am.szczecin.pl

² Space Research Institute, Moscow 117997, Profsoyuznaya St. 82/34, Russia

Key words: radar, microwave scattering, resonant and non-resonant mechanism of scattering, scattering by the breaking waves

Abstract

The paper outlines the radar studies of the sea surface by means of two polarizations X-band radar IKI-2M in Gelendzik, the Black Sea. Observation were performed in “time-distance” regime with azimuthal position of antenna being fixed. The main attention was paid to wave breakings, which have formed the tracks of limited length at the time-distance display. Two kinds of wave breakings are selected: breakings of long gravity waves, moving with velocities 6–8 m/s (“macro-breakings”) and breakings of small-scale meso-waves (“micro-breakings”), which are moving with velocities 0.5–1.0 m/s. The macro-breakings are characterized by sufficiently long time-life about 10–15 s, whereas micro-breakings manifest much shorter times of life about 1–2 s. Probability distributions are obtained for life-times and for characteristic velocities of localized “scattering spots”, observed at the radar images. The analysis of the experimental data allowed distinguishing the resonant and non-resonant mechanisms of scattering.

Słowa kluczowe: radar, rozproszenie mikrofal, rezonansowe i nierezonansowe mechanizmy rozproszenia, rozproszenie na załamujących się falach

Abstrakt

W artykule opisano badania powierzchni morza za pomocą dwupolaryzacyjnego radaru IKI-2M w Gelendziku, Czarne Morze. Obserwacje były przeprowadzone w reżimie „odległość–czas” przy stałym azymucie anteny. Główna uwaga była zwrócona na załamujące się fale, które formowały ślady (treki) ograniczonej długości na dyspleje „odległość–czas”. Dwa rodzaje treków zostały zidentyfikowane jako: załamujące się długie fale, poruszające się z szybkością 6–8 m/s („makrozałamujące się fale”) i załamujące się drobno-skalowe mezo-fale („mikrozałamujące się fale”), których szybkość wynosi 0,5–1,0 m/s. Makrozałamujące się fale charakteryzują się długim czasem życia 10–15 s, natomiast mikrozałamujące się fale mają znacznie krótszy czas życia 1–2 s. Znalezione również rozkłady prawdopodobieństwa dla czasu życia i charakterystycznej szybkości przesunięcia zlokalizowanych centrów rozproszenia, widocznych na radarowych zdjęciach. Analiza eksperymentalnych danych pozwala na rozróżnienie rezonansowych i nierezonansowych mechanizmów rozproszenia.

Introduction

The physical mechanisms of microwave scattering always were in the focus of interests for both experimentalists and theoreticians since the first systematic radar observations of the sea surface in 60-ths. In spite of great efforts, fact is

that experimental values of radar cross-section and Doppler shift of the scattered signal significantly differ from the theoretical estimates, based on commonly accepted two-scale model of the sea surface, which describes back-scattering from small-scale “ripples”, located on the large-scale gravity waves [1, 2, 3, 4, 5].

The main tendency in the interpretation of experimental data consists in introduction the non-resonant (non-Bragg) mechanisms of scattering additionally to the resonant Bragg model. The most known non-resonant mechanism of scattering is connected with the breaking gravity waves (phenomenon of “macro-breaking”). Less known kind of non-Bragg mechanism is realized by the steep and sharp-ended waves of meso-scale spectrum, frequently referred to simply as meso-waves, because their lengths are intermediate between small scale ripples, of few centimeters by length, and large scale gravity waves, longer than 10 m. Breaking meso-waves are responsible for the phenomenon of “micro-breaking”.

Radar IKI-2M

The two polarization high resolution radar was developed in the Space Research Institute of the Russian Academy of Sciences for detailed studying the wave processes on the sea surface. Radar IKI-2M has a wavelength 3 cm (X-band). The pulse duration $T_p = 40$ ns provides radial resolution $\Delta r \approx 6$ m. The pulse power of the emitted signal is about 8 kW. The width of directivity pattern $\Delta\varphi = 1^\circ$ corresponds to azimuthally resolution about 7.5 m at a distance 1 km.

Radar IKI-2M was installed on the roof of the container laboratory on the height 10 m over water surface (Fig. 1). The conversion of analogous radar signals into digital form is performed by 16-degree ADC with frequency 100 MHz. The laboratory container was placed in the end of the long, about 200 m length, mole in the Blue Bay near Gelendzhik (near Novorossiysk, North shore of the Black Sea). Antenna was oriented in the South direction, oppositely to waves, moving mainly to the North.



Fig. 1. Radar IKI-2M, installed on the roof of the container laboratory in the Blue Bay, near Gelendzhik, the Black Sea
 Rys. 1. Radar IKI-2M zainstalowany na dachu kontenera badawczego w Blue Bay niedaleko Galendzik, Morze Czarne

Time-distant regime of radar measurements

The time-distance regime of radar measurements implies fixing antenna’s azimuthal position and registering intensity $I_n(x)$ of the echo signal for every pulse, emitted at discrete time-moments $\tau_n = nT$, $n = 1, 2 \dots$. Here T is a time interval between pulses and x is a distance from the studied area on the sea surface and radar antenna. Mapping the measured intensity $I_n(x)$ on time-distance plane (x, τ) and considering discrete value $\tau = nT$ as continuous variable, we may study the “tracks”, formed on the (x, τ) plane by echo signals from the targets and wave processes on the sea surface.

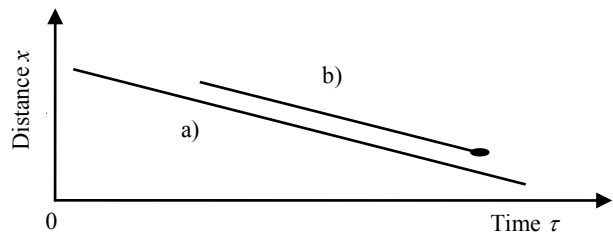


Fig. 2. Rectilinear tracks of long gravity wave on the time-distance plane (x, τ) : a) continuous track, corresponding to uniformly moving gravity wave; b) finite track, corresponding to the breaking gravity wave (“macro-breaking” phenomenon)
 Rys. 2. Prostolinijne ślady fal grawitacyjnych długich na płaszczyźnie czas-odległość (x, τ) : a) ślad ciągły, odpowiadający jednolitemu ruchowi fali grawitacyjnej, b) ślad końcowy, odpowiadający załamującej się fali grawitacyjnej (zjawisko fali załamującej się typu „makro”

The tracks, produced by gravity waves on (x, τ) plane, were studied earlier in the papers [6, 7, 8] for revealing the nonlinear interaction of gravity waves, in particular, for detecting the second harmonics of dominating (energy bearing) waves. In this paper we use time-distance regime for studying finite tracks, answering to the breaking waves on the sea surface.

In the case of point target, moving to antenna with radial velocity v within the main lobe of directivity pattern, echo signal is concentrated near target trajectory $x(\tau)$, which forms a track on the (x, τ) plane. Uniformly moving target forms the straight line trajectory:

$$x = x_0 - v(\tau - \tau_0) \tag{1}$$

where: x_0 is an initial target position at $\tau = \tau_0$.

The long gravity waves, not experiencing breakings manifest themselves on the sea surface by radar signal scattering on small-scale ripples. The surface wave, uniformly moving to antenna with phase velocity v_{ph} , produces on the (x, τ) plane the rectilinear track:

$$x = x_0 - v_{ph}(\tau - \tau_0) \tag{2}$$

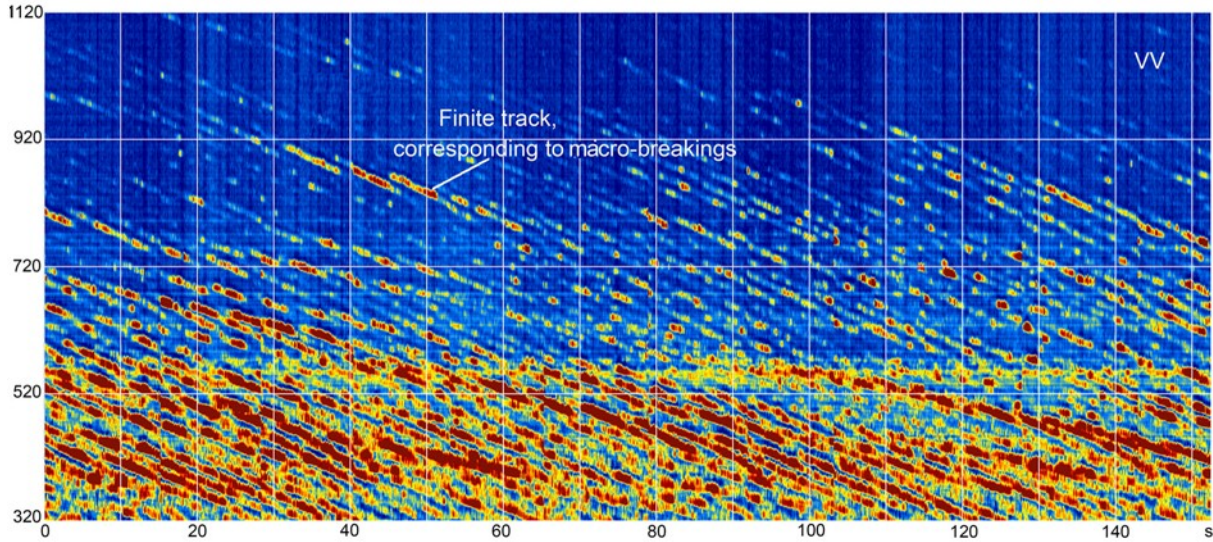


Fig. 3. Finite tracks on the time–distance plane (x, τ), corresponding to breaking of gravity waves, moving with the velocity 6–8 m/s (phenomenon of “macro-breaking”)

Rys. 3. Ślad końcowy na płaszczyźnie czas–odległość (x, τ), odpowiadający załamaniu fal grawitacyjnych poruszających się z prędkością 6–8 m/s (zjawisko fali załamującej się typu „makro”)

This track, presented by continuous straight line a) on figure 1, is similar to the track of the uniformly moving point target, eq. (1). Making use of the dispersion relation:

$$v_{ph}^2 = g/k \quad (3)$$

connecting the phase velocity $v_{ph} = \omega/k$, frequency ω , wave number k and a gravity constant $g = 9.8 \text{ m/s}^2$, one can estimate a dominating wavelength:

$$\lambda_{dom} = \frac{2\pi}{k} = \frac{2\pi}{g} v_{ph}^2 \quad (4)$$

and thereby distinguish the wave packets of different wavelengths. As said, in this paper we use time–distance regime for registration of the breaking waves on the sea surface. Breaking waves manifest themselves by characteristic spot in the end of continuous part of a track on the (x, τ) plane, as schematically shown by the finite line b) at the figure 2.

Observations of finite tracks, corresponding to macro-breakings

Radar images of the sea surface, registered in the time–distance regime, have revealed the continuous and finite tracks on the distance–time plane. The continuous tracks are moving to radar with velocity 6–8 m/s, characteristic for gravity waves of wavelength 10–20 m. At the moment of breaking, the gravity wave gives rise to turbulent water flow, described as the “boiling water state”.

This kind of wave breaking we identify with the phenomenon of “macro-breaking”.

General view of tracks at the radar display is presented at figure 3, which embraces time–interval 125 s and distances 320–900 m. Typical duration of the bright spot in the of track is about 10–15 s, whereas duration of the whole track might be few tens seconds. This duration is comparable with the time of the wave being within directivity pattern.

It seems naturally to assume that the resulting cross–section of the macro–breaking is proportional to the visible area S_{vis} of the water–air turbulent mix:

$$\sigma_{tot} = \chi S_{vis}, \quad \chi \leq 1 \quad (5)$$

where: χ is an averaged reflectivity factor.

Intuitively acceptable phenomenological relation (5) can be illustrated by following qualitative model of scattering. Let the water–air mix consists of randomly positioned water spheres of radius ρ . Because of high conductivity of the sea water in microwave band, we may ascribe cross–section $\sigma_1 = \pi\rho^2$ to every water sphere, similar to metallic sphere. Then total radar cross–section of the turbulent water–air mix is determined by the number N of scattering spheres on the sea surface, which can be estimated as $N = S_{vis} / \pi\rho^2$. It leads to the relation:

$$\sigma_{tot} = N\sigma_1 \approx \sigma_1 S_{vis} / \pi\rho^2 \approx S_{vis} \quad (6)$$

which agrees with eq. (5) for $\chi = 1$.

Proportionality between total cross-section σ_{tot} and visible surface S_{vis} can be derived also for scattering elements of non-spherical form and for elements, obeying statistical distribution. Coefficient of proportionality χ in (5) depends mainly on microwave absorption in the air bubbles. Due to stochastic nature of the turbulent water surface, one may think that the coefficient of proportionality χ in (5) only weakly depends on the radar wavelength, on the angle of incidence and on polarization of the incident wave.

The visual surface S_{vis} of the macro-breaking spot is typically about 10–20 m². Based on the phenomenological relation (5), the radar cross-section σ_{tot} of the macro-breaking also can be estimate by 10–20 m². Such a cross-section causes bright spot in the end of wave track, which visually is 10–20 times brighter as compared with continuous part of track. The later is formed by ripples on the crest of gravity wave, which obey to Bragg mechanism of scattering.

Though incoherent scattering dominates, some elements of macro-breakings may demonstrate the features of coherent scattering. First of all it concerns the sharp-ended water wedges, which might be formed at just before wave's breaking. Let L is the length of the rectilinear wedge. The coherent cross-section of a wedge is estimated as $S_{\text{coh}} \approx L\lambda$, because only λ -vicinity of the water wedge forms the scattered wave. As a result:

$$\sigma_{\text{coh}} \approx \frac{S_{\text{coh}}^2}{\lambda^2} \approx L^2 \quad (7)$$

Thus, rectilinear wedge of 1 m length might give rise to the coherent cross-section of order 1 m², comparable with cross-section of small boat.

The other elements, which may contribute into coherent cross-section, are smooth water flows (water films), arising in the front of macro-breakings. Let R_1 and R_2 be curvature radii of the smooth water film, visible by radar. Then $S_{\text{coh}} \approx \pi R_1 R_2$ and

$$\sigma_{\text{coh}} \approx \frac{S_{\text{coh}}^2}{\lambda^2} \approx \frac{\pi R_1^2 R_2^2}{\lambda^2} \quad (8)$$

For $R_1 \sim R_2 \sim 0.2$ m and $\lambda = 3$ cm this cross-section may reach gigantic value about $\sigma_{\text{coh}} \sim 16$ m², comparable with cross-section of patrol boat.

Effective model of backscattering from the sea surface, containing small ripples and macro-breakings, was suggested recently in the papers [9, 10].

Observations of finite tracks, corresponding to micro-breakings

Besides macro-breakings, our experiments of 2008 have revealed “micro-breakings”, which manifest themselves as series of short finite tracks, which duration is less, than 1 s, as shown at figure 4 for horizontal polarization. Typical velocity of the sea waves, experiencing micro-breaking, is estimated from figure 4 as 0.4–0.6 m/s.

It is reasonable to identify “micro-breakings” with the surface waves of meso-scale (decimeter)

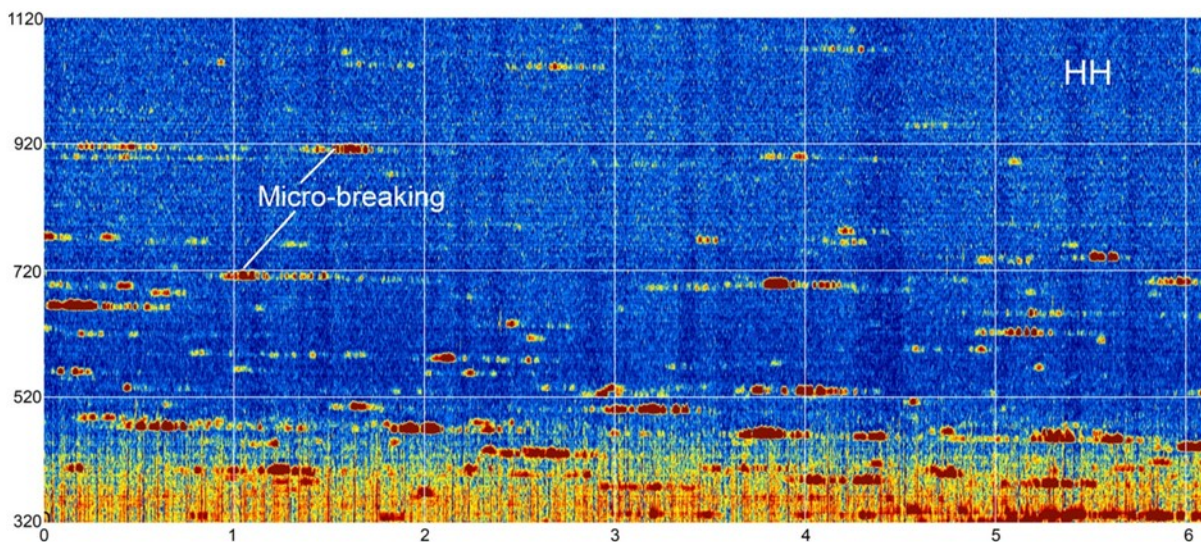


Fig. 4. Micro-breaking phenomenon, observed on the (x, τ) plane in the form of series of short tracks of duration no more than 1 s. Typical velocity of breaking meso-waves is as low as 0.4–0.6 m/s

Rys. 4. Zjawisko załamania fal typu „mikro”, zaobserwowane na płaszczyźnie w postaci serii krótkich śladów trwających nie dłużej niż 1s. Typowa prędkość łamania mezofal osiąga poziom niski 0,4–0,6 m/s

spectrum. They are regarded here as “*meso-waves*”, because their characteristic length 20–30 cm happens to be intermediate between capillary-gravity waves of 1–3 cm length and long gravity waves with wavelength of few meters and longer. Mesowaves arise eventually due to small scale instabilities of the water surface near crest of long gravity waves. As was pointed out in [11, 12, 13, 14, 15, 16], the phenomenon of micro-breakings may play an important role in forming SAR images of the sea surface. Figure 4 presents the first radar observation of mesowaves from small distances. Along with radar observations, the experiments of 2008 have registered also the optical images of mesowaves, which are shown at figure 5.

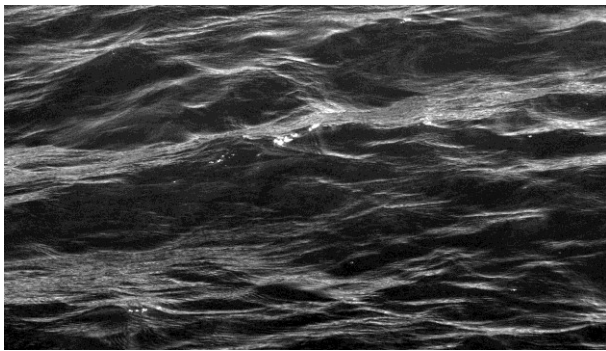


Fig. 5. Optical image of the sharp-ended meso-waves, experiencing “micro-breaking”

Rys. 5. Obraz optyczny gwałtownie zakończonych mezofał, doświadczających „mikrołamania”

The meso-waves break up comparatively quickly after their arising. Therefore the tracks, corresponding to micro-breakings, can be observed no longer than 1–2 s.

Though the waves of meso-scale spectrum, responsible for micro-breakings, have compara-

tively small height about 15–20 cm, comparable with their length, they may cause rather strong echo signal. There are two reasons which increase backscattering. The first one is sharp-crested form of mesowaves just before breaking. The coherent component of radar cross-section, brought about by the sharp-ended crest, is described by eq. (7). Similarly to macro-breakings, the radar cross-section of micro-breakings might be as large as 1 m^2 .

The second factor is the phenomenon of multiple diffractions due to concave shape of the breaking meso-wave. The phenomenon of multiple diffractions can be described in the framework of the geometrical theory of diffraction [16].

Statistical characteristics of backscattering in conditions of „strong” wind

The wave performed two series of observations in 2008–2009, corresponding to “strong” wind (the wind velocity reached 7–8 m/s) and to “weak” wind (velocity was about 5–6 m/s). In conditions of “strong” wind radio images were registered in format $700 \text{ m} \times 300 \text{ s}$, what allowed observing the numerous wave breakings of different duration. Polarization ratio $\sigma_{\text{HH}}/\sigma_{\text{VV}}$ was 1.47. The amount of scattering spots was 450 for horizontal polarization and 512 for vertical one.

Distributions of time-life for horizontal and vertical polarizations are presented at figure 6.

Distributions for velocity of scatterers, measured from the tracks slope at distance-time plane are shown at figure 7 for vertical and horizontal polarizations respectively. The width of velocity distribution for horizontal polarization (Fig. 7b) happened to be two-times wider than at vertical one (Fig. 7a).

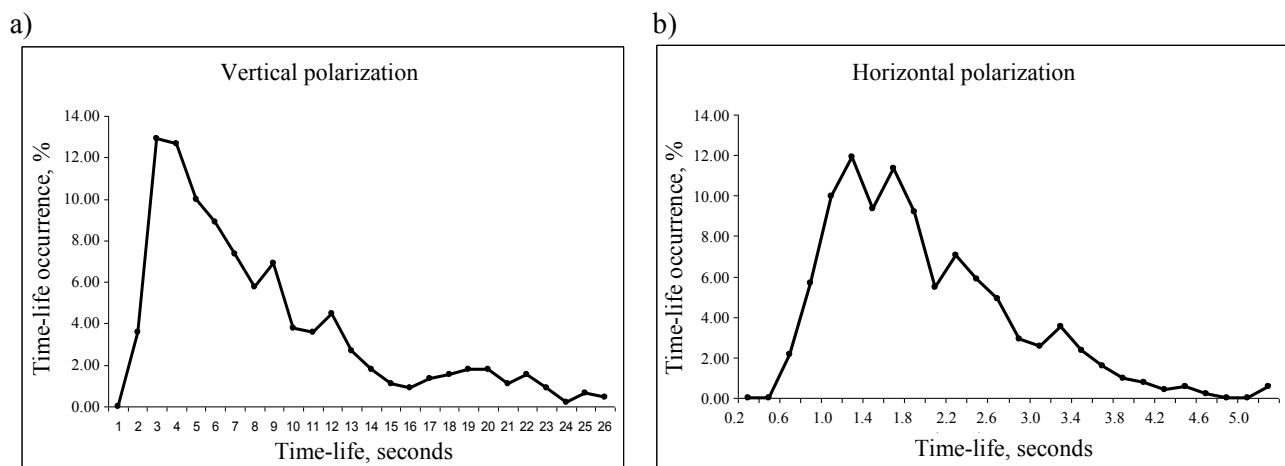


Fig. 6. Time-life occurrence for vertical (a) and for horizontal (b) polarizations in conditions of “strong” wind observations

Rys. 6. „Czas życia” dla pionowych i poziomych polaryzacji w warunkach silnego wiatru (w warunkach obserwacji przy silnym wietrze)

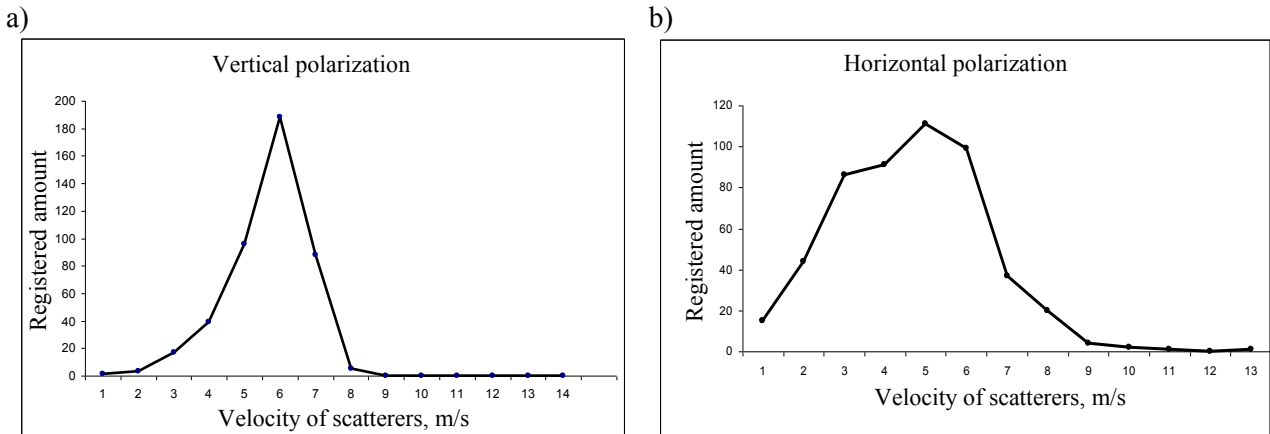


Fig. 7. Distribution of velocities, measured at vertical (a) and at horizontal (b) polarizations for “strong” wind conditions
 Rys. 7. Rozkład prędkości mierzonej dla pionowych (a) i poziomych (b) polaryzacji w warunkach silnego wiatru

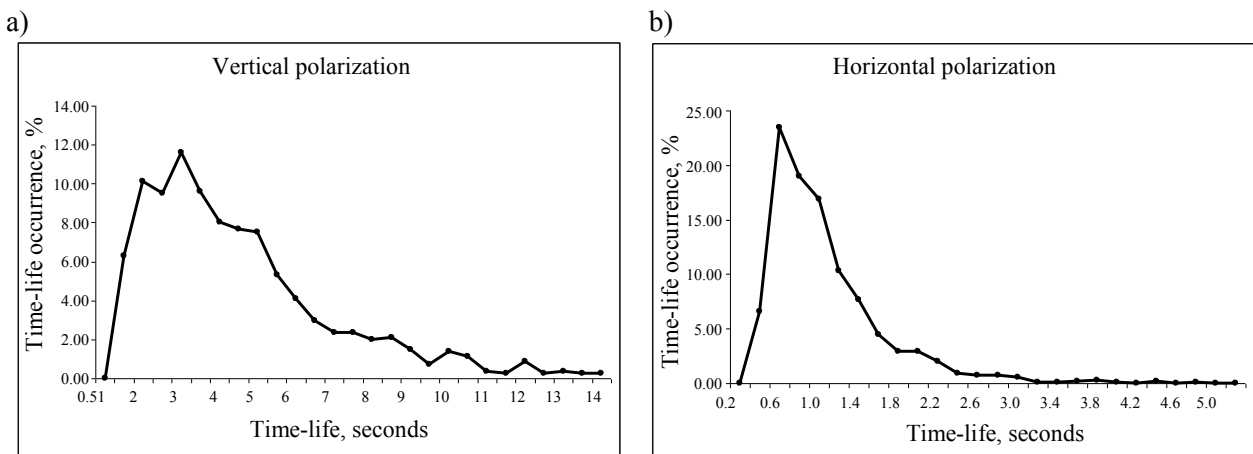


Fig. 8. Time-life occurrence for vertical (a) and horizontal (b) polarizations (“weak” wind series)
 Rys. 8. „Czas życia” dla pionowych (a) i poziomych (b) polaryzacji (seria „słabych” wiatrów)

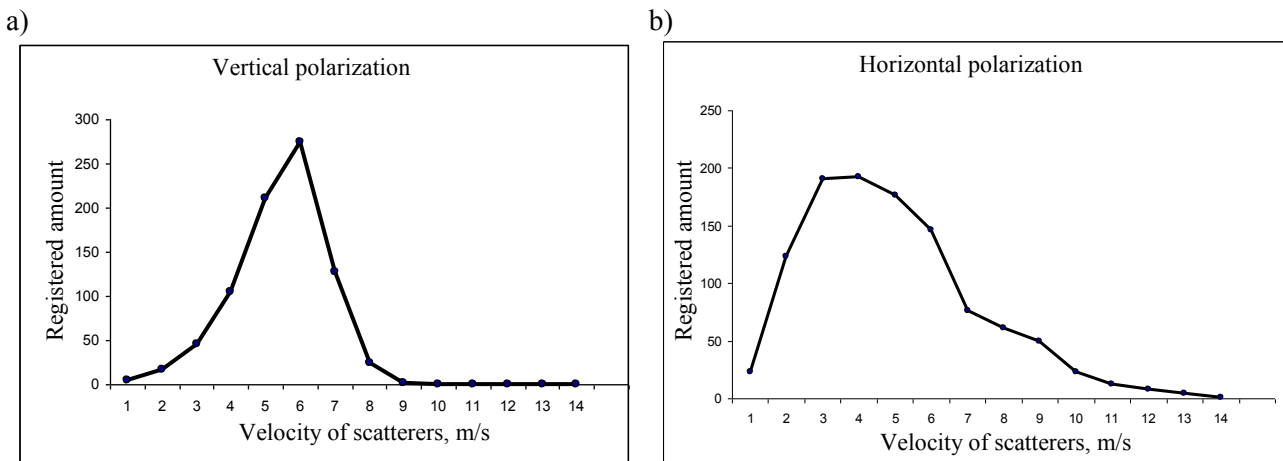


Fig. 9. Distribution of velocities of scatterers, measured at vertical (a) and horizontal (b) polarizations for “weak” wind conditions
 Rys. 9. Rozkład prędkości fal rozproszonych, mierzonych dla pionowych (a) i poziomych (b) polaryzacji w warunkach słabego wiatru

Statistical characteristics of backscattering in conditions of “weak” wind

The second series of observations, which was performed for “weak” wind velocity, dealt mainly with micro-breakings, because macro-breakings

practically were not observed at the low wind velocities about 5–6 m/s. Polarization ratio decreases for weak wind to $\sigma_{HH}/\sigma_{VV} = 0.92$. Format of radio image in the second series was 700 m × 500 s. Amount of scattering spots was 811 at

vertical polarization and 1157 for horizontal one. Distributions of time life are shown at figure 8.

The non-resonant component of scattered signal manifests itself by distinction in velocity distributions, measured at vertical and horizontal polarization. At horizontal polarization, figure 7b, rather slow waves were detected, which phase velocities were as low, as 3 m/s. Corresponding water wavelength is about 5 m, what is less than radar resolution. Detecting of so low velocities can be explained by significant level of signal, scattered at sharp crests of meso-waves. This level was typically at 10 dB higher as compared with background scattering of Bragg nature.

Figure 9 presents distributions of velocities for vertical and horizontal polarizations in conditions of “weak” wind.

Conclusions

1. Radar studies of the sea surface, presented above, have revealed two kinds of breaking waves, qualified as macro- and micro breakings.

2. Statistical characteristics of echo signals from breaking waves were obtained, including distribution of time-life and of scatterer’s velocity. These distributions were registered in conditions of strong and weak winds and for vertical and horizontal polarizations.

3. It is shown that radar cross-sections of the macro-breakings may be comparable with the cross-sections of patrol boats, what should be taken into account under development of security system for maritime ports. The main problem in this problem is distinguishing the small targets from wave breakings. One of the ways for reducing harmful influence of echo signals from macro-breakings is to apply correlation methods of signal processing, based on experimental distributions of time-life.

References

1. BECKMAN P., SPEZICINO A.: The Scattering of Electromagnetic Waves from Rough Surface. Pergamon Press, NY 1963.
2. ISHIMARU A.: Wave Propagation and Scattering in Random Media. Academic Press, NY 1978.
3. BASS F.G., FUKS I.M.: Wave Scattering from Statistically Rough Surfaces. Pergamon Press, Oxford 1979.
4. RYTOV S.M., KRAVTSOV YU.A., TATARSKII V.I.: Principles of Statistical Radio Physics. Vol. 4: Wave Propagation through Random Media. Springer-Verlag, Berlin 1989.
5. VORONOVICH A.G.: Wave Scattering from Rough Surfaces. Springer-Verlag, Berlin 1994.
6. BULATOV M.G., RAEV M.D., SKVORTSOV E.I.: Radar observations of the nonlinear wave processes in the coastal zone. The Third All-Russia Open Conference “Modern problems of the remote sensing of the Earth from the space”. Moscow, the Space Research Institute of the Russian Academy of Sciences, 14–17 November 2005, Proceedings, 50–55.
7. BULATOV M.G., RAEV M.D., SKVORTSOV E.I.: Study of nonlinear waves on the basis of the spatial–frequency spectra of the radar images of the sea surface. The Earth Studies from the Space, 2006, 2, 64–70.
8. BULATOV M.G., RAEV M.D., SKVORTSOV E.I.: Return waves on the sea surface. Physics of Wave Phenomena (Allerton Press, Inc.) 2008, 16(1), 70–75.
9. KUDRYAVTSEV V., HAUSER D., CAUDAL G., CHAPRON B.: A semi-empirical model of the normalized radar cross section of the sea surface. Part 1. Background model. J. Geophys. Res., 2003, 108 (C3).
10. KUDRYAVTSEV V., AKIMOV D., JOHANNESSEN J.A., CHAPRON B.: On radar imaging of current features. Part 1: Model and comparison with observations. J. Geoph. Res., 2005, 110, C07016.
11. KRAVTSOV YU.A., MITYAGINA M.I., CHURYUMOV A.N.: Non-resonant mechanism of electromagnetic waves scattering by sea surface: scattering by steep sharpened waves, Radio Phys. Quant. Electron., 1999, 42(3), 216–228.
12. KRAVTSOV YU.A., MITYAGINA M.I., CHURYUMOV A.N.: Electromagnetic waves backscattering by meso-scale breaking waves on the sea surface, Bull. Russ. Acad. Sci. Phys., 1999, 63(12), 1859–1865.
13. CHURYUMOV A.N., KRAVTSOV YU.A.: Microwave backscatter from mesoscale breaking waves on the sea surface, Waves in Random Media, 2000, 10(1), 1–15.
14. CHURYUMOV A.N., KRAVTSOV YU.A., LAVROVA O.YU., LITOVCHENKO K.Ts., MITYAGINA M.I., SABININ K.D.: Signatures of resonant and non-resonant scattering mechanisms on radar images of internal waves. Int. J. Remote Sens., 2002, 23(20), 4341–4355.
15. BULATOV M.G., KRAVTSOV YU.A., LAVROVA O.YU., LITOVCHENKO K.Ts., MITYAGINA M.I., RAEV M.D., SABININ K.D., TROKHIMOVSKII YU.G., CHURYUMOV A.N., SHUGAN I.V.: Physical mechanisms of aerospace radar imaging of the ocean. Physics-Uspekhi, 2003, 46(1), 63–79.
16. KRAVTSOV YU.A., NING YAN ZHU: Multiple diffraction of electromagnetic waves at a wedge of concave shape. Wave Motion, 2006, 43, 206–221.

Recenzent:

*prof. dr hab. inż. Andrzej Stateczny
Akademia Morska w Szczecinie*